MARTIN MARIETTA ENERGY SYSTEMS LIBRARIES

3 4456 0269087 1

ORNL/TM-10667

ornl

OAK RIDGE NATIONAL LABORATORY

MARTIN MARIETTA

The Influence of the Fiber-Matrix Bond on the Mechanical Behavior of Nicalon®/SiC Composites

R. A. Lowden
D. P. Stinton

OAK RIDGE NATIONAL LABORATORY
CENTRAL RESEARCH LIBRARY
CIRCULATION SECTION
4500N ROOM 175
LIBRARY LOAN COPY
DO NOT TRANSFER TO ANOTHER PERSON
If you wish someone else to see this report, send in name with report and the library will arrange a loan.

Fossil Energy Program

OPERATED BY
MARTIN MARIETTA ENERGY SYSTEMS, INC.
FOR THE UNITED STATES
DEPARTMENT OF ENERGY

Printed in the United States of America. Available from
National Technical Information Service
U.S. Department of Commerce
5285 Port Royal Road, Springfield, Virginia 22161
NTIS price codes—Printed Copy: A04 Microfiche A01

This report was prepared as an account of work sponsored by an agency of the United States Government. Neither the United States Government nor any agency thereof, nor any of their employees, makes any warranty, express or implied, or assumes any legal liability or responsibility for the accuracy, completeness, or usefulness of any information, apparatus, product, or process disclosed, or represents that its use would not infringe privately owned rights. Reference herein to any specific commercial product, process, or service by trade name, trademark, manufacturer, or otherwise, does not necessarily constitute or imply its endorsement, recommendation, or favoring by the United States Government or any agency thereof. The views and opinions of authors expressed herein do not necessarily state or reflect those of the United States Government or any agency thereof.

ORNL/TM-10667

THE INFLUENCE OF THE FIBER-MATRIX BOND ON THE MECHANICAL BEHAVIOR OF NICALON®/SiC COMPOSITES

R. A. Lowden
D. P. Stinton

Date Published - December 1987

NOTICE: This document contains information of a preliminary nature. It is subject to revision or correction and therefore does not represent a final report.

Prepared for DOE Office of Fossil Energy

Prepared by the
OAK RIDGE NATIONAL LABORATORY
Oak Ridge, Tennessee 37831
operated by
MARTIN MARIETTA ENERGY SYSTEMS, INC.
for the
U.S. DEPARTMENT OF ENERGY
under contract DE-AC05-84OR21400

MARTIN MARIETTA ENERGY SYSTEMS LIBRARIES
3 4456 0269087 1

CONTENTS

ABSTRACT 1

1. INTRODUCTION 1

2. EXPERIMENTAL PROCEDURES 2

2.1 COMPOSITE FABRICATION 2

2.2 FLEXURE TESTING 3

2.3 FIBER-MATRIX BOND MEASUREMENTS 7

2.3.1 Indentation Techniques 7

2.3.2 Tensile Testing 10

3. RESULTS 15

3.1 MECHANICAL BEHAVIOR 15

3.2 INDENTATION TESTING 17

3.3 FRAGMENTED COATINGS ON INDIVIDUAL FILAMENTS 17

4. DISCUSSION 21

4.1 PRECOATING AND FRACTURE BEHAVIOR 21

4.2 INTERFACIAL FRICTION 30

5. CONCLUSIONS 32

6. ACKNOWLEDGMENTS 33

7. REFERENCES 33

THE INFLUENCE OF THE FIBER-MATRIX BOND ON THE MECHANICAL BEHAVIOR OF NICALON®/SiC COMPOSITES*

R. A. Lowden and D. P. Stinton

ABSTRACT

The effect of thin coatings deposited on Nicalon fibers prior to densification with silicon carbide by chemical vapor infiltration was investigated. The thin films were applied to alter the strength of the fiber-matrix bond and to protect the fibers during processing. An indentation method developed to measure the strength of fiber-matrix bonding and frictional stresses was investigated and compared to a simple tensile test technique. The influence of the coatings on the bond strength and mechanical behavior of the composite products was examined.

1. INTRODUCTION

Many ceramic matrix composites reinforced with ceramic fibers have been shown to have improved mechanical behavior compared with conventional ceramics.[1-4] High strength ceramic fibers incorporated into brittle matrices will typically increase fracture toughness and prevent catastrophic failure. The increase in toughness is a result of a number of energy absorbing mechanisms that are controlled by the strength of the fiber-matrix bond. Brittle failure in ceramic composites, characterized by flat fracture surfaces and a lack of fiber pull-out, is attributed to an excessively strong fiber-matrix bond. Debonding, crack deflection, and fiber pull-out all contribute to improve fracture toughness; they are dependent upon a weak bond at the fiber-matrix interface.[5-9]

®Nippon Carbon Company, Tokyo, Japan.

*Research sponsored by U.S. Department of Energy, AR&TD Fossil Energy Materials Program [DOE/FE AA 15 10 10 0, Work Breakdown Structure Element ORNL-1(C)] under contract DE-AC05-84OR21400 with Martin Marietta Energy Systems Inc.

Quantitative analysis of the interfacial bond strength and frictional stresses and detailed characterization of the chemical interactions at the fiber-matrix boundary are essential to establish a correlation relating composite properties to interfaces. When the nature of the fiber-matrix interface is fully understood, interfacial pretreatments can be employed to control fiber-matrix bonding and interaction, and ultimately the mechanical behavior of composite materials. Interfacial coatings or treatments to modify fiber-matrix bonding have been examined with positive results.[10 11] Thin films have been deposited on fiber surfaces to weaken the fiber-matrix interface, therefore enhancing fiber pull-out and slip. This has resulted in increased toughness and ultimate strength of the composite materials.

Fiber coatings may prove useful in other areas of concern in fiber-reinforced composites. Thin films deposited on the fiber surfaces may protect the reinforcement from damage during processing. For example, a thin pyrolytic carbon layer deposited on fibrous preforms prior to densification increased product reproducibility and improved mechanical properties in Nicalon/SiC composites fabricated using chemical vapor infiltration (CVI) techniques.[12] Precoating fibers prior to matrix deposition can also provide protection from chemical attack by the matrix or from environments encountered during both processing and actual use.

This report describes a study of fiber coatings used to alter the fiber-matrix bond and change the mechanical behavior of a ceramic fiber-reinforced ceramic matrix composite. The strength of the fiber-matrix bond was determined using established indentation methods[13] and a simple tensile test that is currently under development. The flexure strengths and resulting fracture behavior were used to qualitatively compare the effects of the various fiber pretreatments.

2. EXPERIMENTAL PROCEDURES

2.1 COMPOSITE FABRICATION

Fibrous preforms were fabricated by stacking multiple layers of plain-weave SiC cloth rotated in a 30°-60°-90° sequence within the cavity of a graphite holder. The layers were hand compressed and held in place by a

perforated graphite lid pinned to the holder. The cloth sizing was removed through multiple washings in acetone. The average fiber content of the resulting fiber preforms was 41.4 ± 1.3 vol% with sample dimensions of 45 mm diameter and 12.5 mm thickness.

The preforms were next precoated with thin layers of various materials. The deposition parameters and nominal thicknesses of the films are summarized in Table 1. The presence of the coatings was verified using X-ray line scan and dot map data obtained using a JEOL 733 electron microprobe (Fig. 1). A control sample of uncoated fibers was prepared for comparison.

The coated preforms were densified using the forced-flow, thermal gradient, chemical vapor infiltration (FCVI) process developed at ORNL.[14-16] The composites were infiltrated with SiC produced by the decomposition of methyltrichlorosilane (MTS) in hydrogen. The deposition parameters used were as follows: a top surface temperature of 1200°C, an MTS flow of 0.333 g/min, a hydrogen flow of 500 cm^3/min, and atmospheric pressure.

The infiltrated composite samples had an average bulk density of 2.78 ± 0.19 g/cm^3, which is approximately 95% of theoretical density. The theoretical density is defined as the sum of the products of volume fraction and reported density of the components of the composite (fibers; precoat; and, after infiltration, SiC). These values are calculated directly from measured weight gain and are used only as a preliminary evaluation of the infiltration process.

2.2 FLEXURE TESTING

Twelve bend bars were prepared from each sample [four each from the top, middle, and bottom areas (Fig. 2)] to determine variations within and between samples. The bars were cut from the samples parallel to the 0°-90° orientation of the top layer of cloth using a diamond saw, and tensile and compression surfaces were ground parallel to the long axis of the specimen. The average dimensions of the bars were 2.5 × 3.3 × 45 mm; all were measured and weighed to determine densities.

Flexural strengths were measured at room temperature using four-point bending methods, with a support span of 25.4 mm, a loading span of 6.4 mm,

Table 1. Preform processing parameters

Sample	Fiber content (%)	Precoat[a]	Reactant gas	Diluent gas	Top surface temperature (K)	Calculated precoat thickness (μm)[b]	Infiltration time (h)
170	41.8	Silicon	15 cm^3/min SiH_4	500 cm^3/min Ar	675	0.17	24.8
171	41.3	Pyrocarbon	10 cm^3/min C_3H_6	500 cm^3/min Ar	1375	0.03	21.3
172	42.1	Boron	15 cm^3/min B_2H_6	500 cm^3/min Ar	775	0.50	26.1
173	39.0	Silicon carbide	25 cm^3/min CH_3SiH_3	500 cm^3/min Ar	1125	0.08	23.7
174	41.8	Pyrocarbon	20 cm^3/min C_3H_6	500 cm^3/min Ar	1375	0.12	21.7
175	43.5	Pyrocarbon	15 cm^3/min C_3H_6	500 cm^3/min Ar	1375	0.07	22.0
176	42.0	Silicon carbide	25 cm^3/min CH_3SiH_3	500 cm^3/min Ar	975	0.22	22.5
177	40.4	Boron nitride	15 cm^3/min B_2H_6	40 cm^3/min NH_3	875	0.13	20.6
178	40.3	Uncoated		500 cm^3/min Ar	1375		21.7

[a]All precoat times 2 h.

[b]Calculated from weight gain.

YP-4969

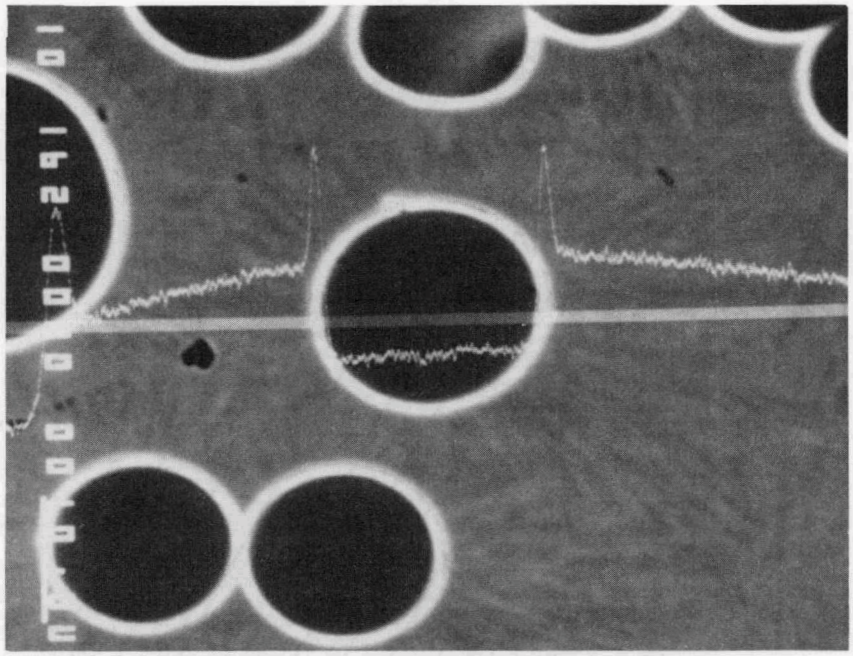

(a)

YP-4972

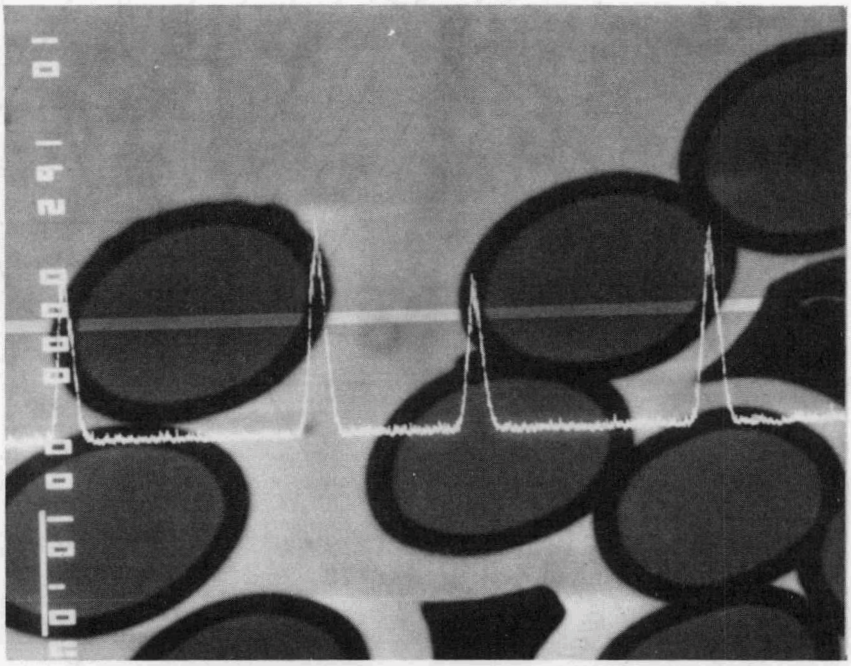

(b)

Fig. 1. The presence of the thin films was verified using microprobe line scan data. (*a*) Silicon coating on Nicalon fibers in SiC matrix. (*b*) Boron coating on Nicalon fibers in SiC matrix.

ORNL-DWG 87-14913

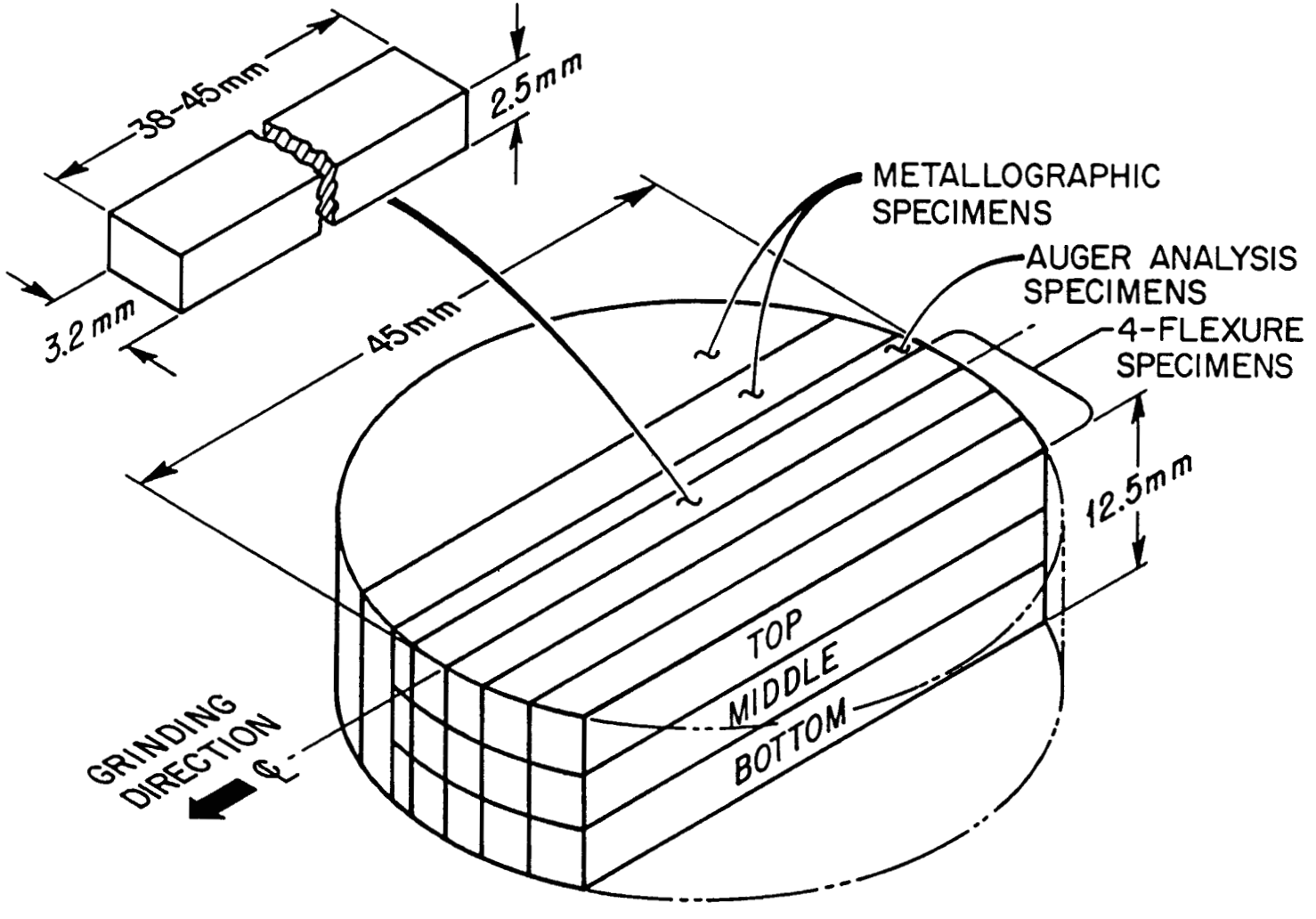

Fig. 2. Location of test specimens within sample.

and a crosshead speed of 0.051 cm/min. Specimens were loaded perpendicular to the layers of cloth. The fracture surfaces of the specimens were examined using both a Hitachi S-800 and JEOL JSM-35CF scanning electron microscopes. Specimens that did not completely fracture during flexure testing were broken by hand so that the fracture surfaces could be examined.

2.3 FIBER-MATRIX BOND MEASUREMENTS

2.3.1 Indentation Techniques

Several methods to quantify the strength of interfacial bonding in fiber-reinforced composites have been developed.[13,17,18] These have involved either pushing or pulling on individual fibers embedded in a continuous matrix and determining the required forces. Such tests permit a quantitative determination of the bond strength and interfacial frictional stresses, derived from relatively simple load and displacement relationships.

The indentation method for measuring interfacial bonding forces has been thoroughly examined. This technique involves using a microhardness indentor to apply a force to the end of a fiber embedded in a matrix (Fig. 3). The bond strength can be calculated from the applied load and the displacement of the fiber.

Marshall's analysis[13] of the forces needed to displace a fiber in a thin specimen yields

$$F = 2\pi R t \tau \ ,$$

where τ is the frictional stress, t is the thickness of the sample parallel to the direction of the fibers, and R is the fiber radius. This relationship holds for thin specimens in which the thickness of the sample is less than the sliding distance of the fiber. The fiber will thus simply be pushed out of the opposite surface when a load is applied. The analysis becomes much more complex if the thickness of the specimen is larger than the sliding distance; however, it can be approximated that the given relationship can be applied to thicker specimens if the thickness of the specimen is much greater than the sliding distance. The frictional stress

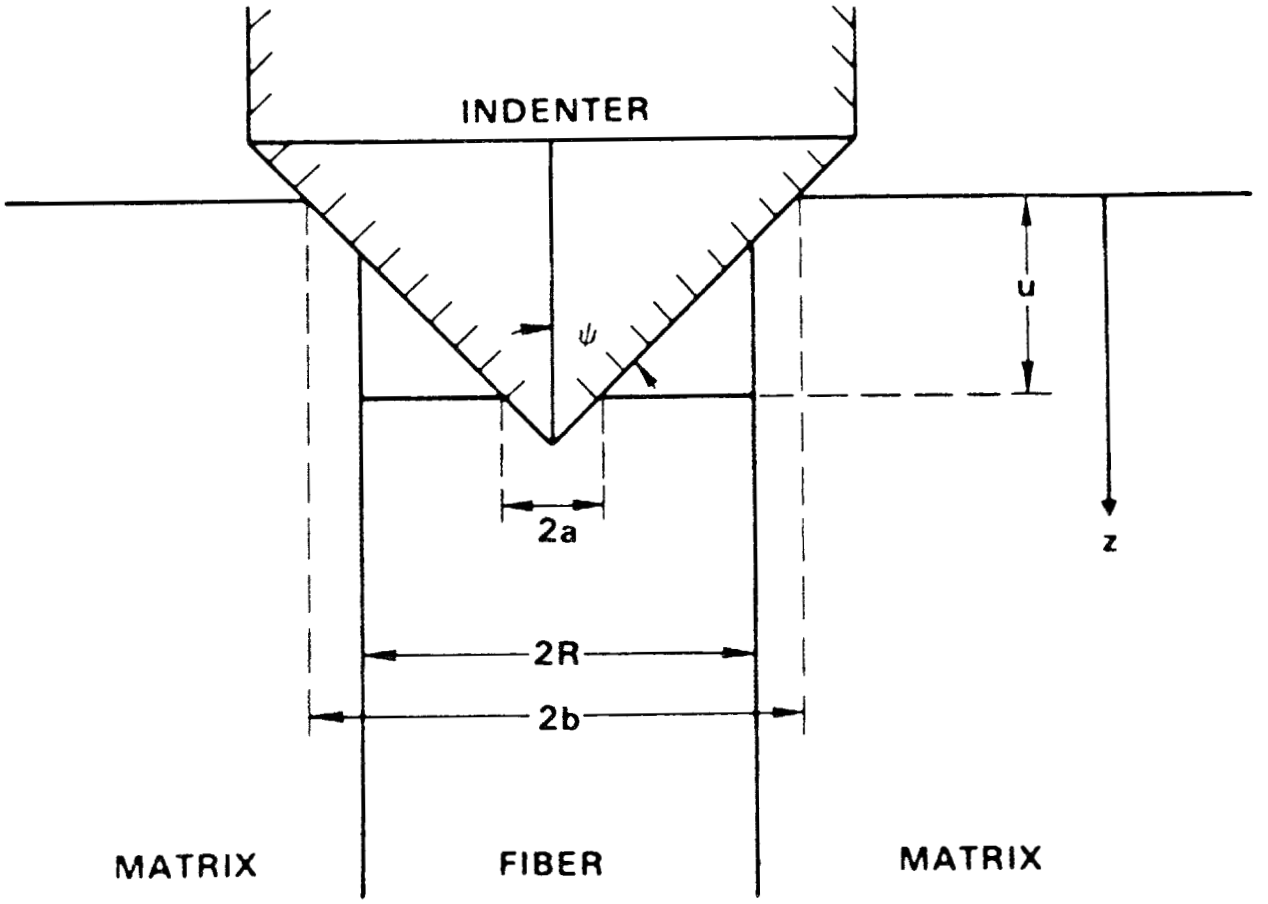

Fig. 3. Schematic of indentation method for measurement of fiber-matrix friction stress. *Source:* D. B. Marshall, "An Indentation Method for Measuring Matrix-Fiber Frictional Stresses in Ceramic Components," *Comm. Amer. Ceram. Soc.* C259-60 (December 1984).

can then be calculated from the displacement of the fiber, u, due to the load imposed by the diamond indentor. The frictional stress is

$$\tau = F^2/4\pi^2 uR^3 E_f \ ,$$

where E_f is the Young's modulus of the fiber and u is the fiber displacement. The value of u can be determined from the indent impression dimensions, a and b, and the indentor angle, ψ, as shown in Fig. 3,

$$u = (b-a) \cot \psi/2 \ .$$

The force supported by the fiber, F, can be obtained from hardness impressions on the fiber,

$$F = 2a^2 H \ ,$$

where H is the hardness of the fiber.

A more comprehensive determination of the forces and displacements that occur in an indentation test is possible using the ultralow load Nanoindentor.[19-21] A coil and magnet assembly is used to move the indentor and apply loads; thus, load and displacement can be accurately measured with resolutions of 0.3 uN and 0.16 nm. Some interesting results have been obtained from studies of the response of an embedded fiber to cyclic loading and unloading. The fact that the instrument is limited to loads of 0.12 N loading rates of 10 nm/s may limit its usefulness to research scale testing and experimentation.

Coyle and Fuller at the National Bureau of Standards have completed preliminary work on fiber-matrix debonding and frictional sliding using an instrumented hardness indentor.* As compared to the Nanoindentor, the device is capable of applying load up to 20 N; it simultaneously records load and displacement. The instrument can apply higher loads, is lower in cost, and is simpler to operate. Further evaluation of the instrument will be necessary before its applicability can be determined.

---

*Personal communication with T. Coyle, National Bureau of Standards, Gaithersburg, MD.

A 6.0-mm-thick cross-sectional specimen was cut from each completed composite sample to be used for indentation testing. The specimens were cut along the 0-90° orientation of the top layer of cloth to ensure that a portion of the exposed fibers would be oriented perpendicular to the cut surface. This alignment is essential for proper implementation of the indentation mechanics. The specimens were mounted and polished using standard metallographic techniques. Loads were applied to fiber ends using a Vickers diamond indentor and a Shimadzu Type M instrument.† Loading to the fiber ends was progressively increased until debonding was observed and then again until contact of the indentor with the edge of the fiber cavity was evident. Loads of up to 300 g were required to displace the fibers.

2.3.2 Tensile Testing

Although indentation techniques can promote a better understanding of the nature of the interface and its role in the behavior of fiber-reinforced materials, these "push tests" are complicated by several factors. The Poisson expansion of the fiber due to compressive loading, the nature of the indentor penetration into the fiber end, and the intricacies of a completed composite specimen all add to the complexity of the analysis. In addition, the samples must first be cut, ground, and polished prior to testing, most likely disturbing the fiber-matrix interface. It has been postulated that a less complex method employing a simple tensile test could be developed to examine interfacial phenomena.[22-24]

During mechanical property evaluation of Nicalon fiber-reinforced/SiC matrix composites fabricated using FCVI techniques, segmental fracturing of the fiber coatings on the tensile side of flexure specimens was observed. An example of this fracture phenomenon is shown in Fig. 4. Based on the multiple matrix cracking concepts described by Aveston, Cooper, and Kelly[25,26] and some recent work by Drzal[27] on interfaces in polymer matrix-graphite fiber composites, a simple tensile test to determine interfacial frictional stress was devised.

In general, the fibers in a ceramic-ceramic composite have a higher strain to failure than that of the matrix, and it is assumed that the

---

†Shimadzu Corporation, Tokyo, Japan.

ORNL-PHOTO 0156-87

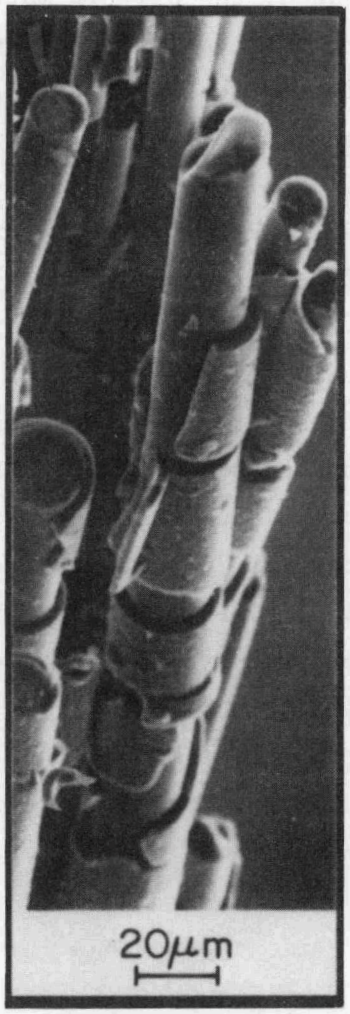

Fig. 4. Segmental fracture of coatings on tensile side of flexure specimens.

ceramic matrix materials are essentially inelastic. When a ceramic-ceramic composite is stressed, the brittle matrix will fail before the fibers. In the event of matrix failure, the load is transferred from the matrix to the fibers. If the fibers are of high strength, they will not fail. As loading continues the fibers will strain, and multiple cracking of the matrix will occur.

A method has been developed to take advantage of the preceding observations to measure fiber-matrix bonding. A thin coating is deposited on a section of a single filament. The filament is then gripped on the uncoated ends, and a tensile force is applied [Fig. 5(*a*)]. Load transfer to the coating from the fiber can only occur across the fiber-matrix interface. As loading continues, the axial stress in the coating increases until the coating fractures circumferentially [Fig. 5(*b*)]. Continued application of the load results in repeated fracture of the coating into uniform lengths [Fig. 5(*c*)]. The lengths of these fragments is dependent upon the interfacial frictional stress, the rupture strength of the coating, and the thickness of the film.

From an equilibrium of forces between the axial stress in the coating, σ_{cg}, and the interfacial shear stress, τ_i, acting on length $\ell/2$ (because the fiber is loaded from both ends), a simple relationship can be derived:

$$\sigma_{cg} = F/A_{cg} ,$$

where F is the applied force and A_{cg} is the area of the coating given by $A_{cg} = \pi (d_c^2 - d_f^2)/4$. The diameter of the coating is d_c, and the diameter of the fiber is d_f. The shear stress at the interface is

$$\tau_i = F/A_f ,$$

where A_f is the surface area of the fiber, $A_f = \pi d_f \ell/2$. Setting the forces equal

$$\sigma_{cg} A_c = \tau_i A_f$$

$$\sigma_{cg} \pi (d_c^2 - d_f^2/4 = \tau_i \pi d_f \ell/2 ;$$

ORNL DWG 87-1999

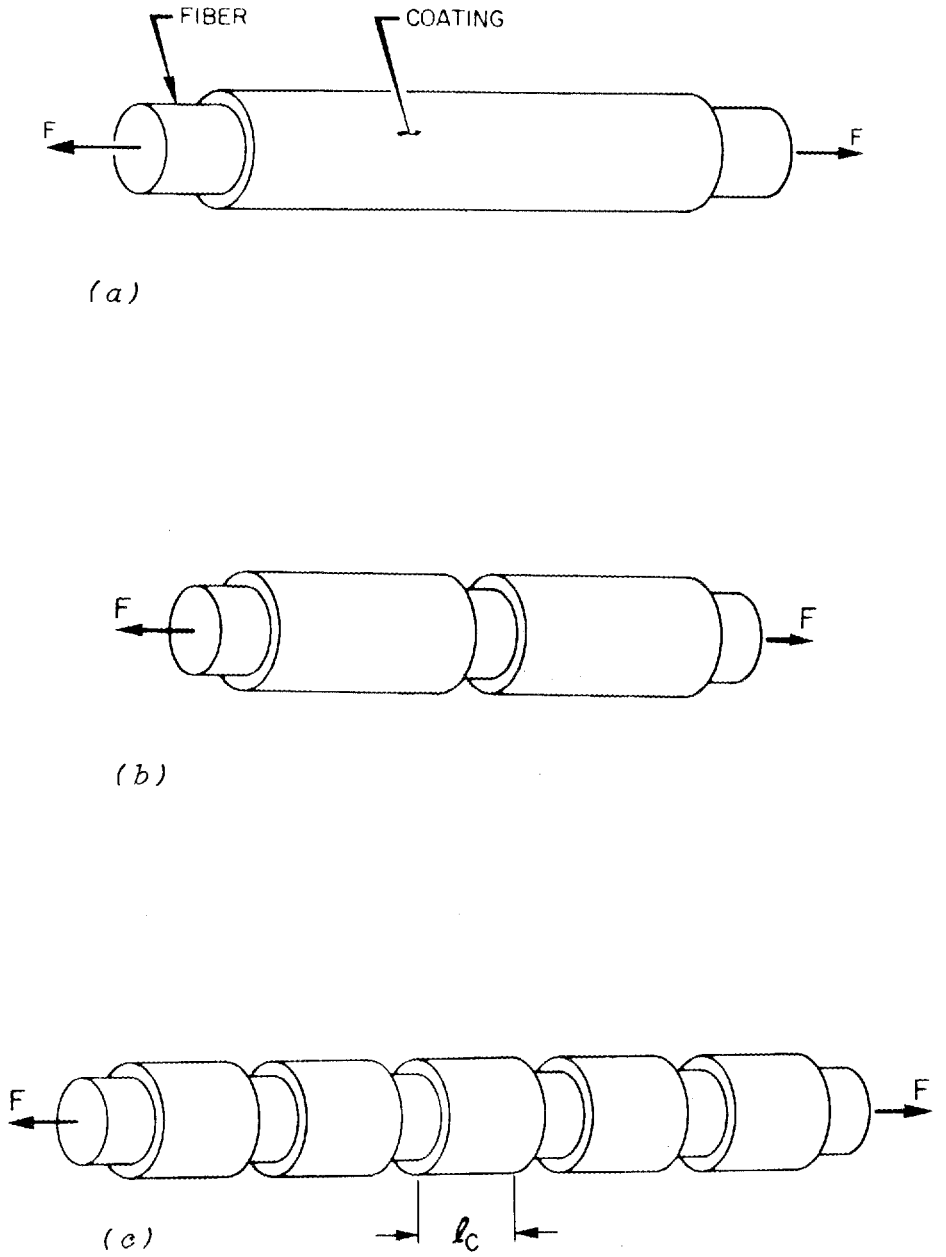

Fig. 5. The sequence of coating fracture as loading is increased.

and solving for shear,

$$\tau_i = \sigma_{cg} (d_c^2 - d_f^2)/2\, d_f\, \ell_c ,$$

where ℓ_c is the critical length of a fracture segment.

From the interfacial shear strength equation it can be concluded that high shear stress results in short critical lengths, while low shear stresses result in longer critical lengths. In order to examine the feasibility of this approach, thin coatings were applied to the center section of individual filaments using chemical vapor deposition techniques. In an initial series of experiments, a 10.0-μm coating of silicon carbide was deposited on untreated large diameter (140-μm) AVCO SCS-6 filaments.* The filaments were glued into graphite fixtures using a high-temperature graphite cement and were hung in the hot zone of a resistively heated furnace. The coating was applied to 15-cm lengths of the filaments by decomposing MTS in the presence of excess hydrogen at 1475 K and a pressure of 13.3 KPa. The reactant gases were introduced such that deposition occurred only on the center sections of the fibers.

The coated fibers were removed and placed in a small tensile frame for loading in tension. The load was applied by hand using a fine thread micrometer head, and the fibers were observed during loading using a low power stereoscopic microscope. Tension was increased until repeated fragmentation of the coating was observed. The tension was held constant, and the critical lengths of the fractured sections were measured from photographs and by using the ocular scale of the microscope. It was necessary to hold the fibers in tension while the fragments were examined, because releasing the load resulted in closing of the cracks. In addition, if the segments slipped during stressing, sections of the coating buckled and spalled.

The procedure was repeated for filaments precoated with a <1.0-μm-thick film of pyrolytic carbon. The pyrocarbon layer was deposited on the

---

*AVCO Specialty Materials Division, Lowell, MA.

filaments from a mixture of 25 cm^3/min propylene gas in 500 cm^3/min argon at 1375 K and a pressure of 3 KPa. A 10-μm SiC coating was then applied employing the previously described fixturing and procedures. The coated filaments were tested, and critical lengths were recorded.

The same methods were applied to Nicalon fiber tows. Yarns wereplaced in holders and coated first with SiC and then with pyrolytic carbon and SiC. The SiC deposition pressure was reduced to 3 KPa to produce uniform coatings throughout the fiber bundles. The fiber tows were tested, and segment lengths were measured from photographs at a magnification of 320X. Uniform loading of each individual filament within the entangled yarns was impossible, and fusion of filaments at contact points during coating compounded the difficulty.

It was recognized that the procedure could be easily and routinely implemented only by using individual filaments. Graphite mounting fixtures similar to those described in ASTM standard for tensile testing brittle fibers have been fabricated. The holders, designed to provide support for fragile single filaments, have been miniaturized to fit into the chamber of the JEOL 35CF scanning electron microscope. The stage of the microscope is capable of applying a tensile load to small specimens. The sequential fragmentation of thin films on individual Nicalon filaments will be examined in the SEM in the future.

3. RESULTS

3.1 MECHANICAL BEHAVIOR

The four-point flexure strengths of the composite specimens are summarized in Table 2. The data are listed by position in order to correlate density variations in the composite samples due to nonuniform infiltration. Density affects both flexure strength and fracture behavior. The difficulties in applying flexure tests to composites are recognized, and the results are reported for comparison rather than as actual tensile strength values. Load-crosshead displacement curves were recorded and were used to examine fracture phenomena.

Table 2. Property summary for composites specimens

Sample	Position	Density (g/cm^3)	T.D. (%)	Flexure strength (MPa)
170	Top	2.43 ± 0.03	83.5 ± 1.0	99.0 ± 4.1
	Middle	2.35 ± 0.03	80.9 ± 1.0	82.2 ± 15.5
	Bottom	2.28 ± 0.03	78.4 ± 1.2	82.7 ± 3.9
171	Top	2.48 ± 0.03	85.3 ± 0.9	109.5 ± 9.7
	Middle	2.36 ± 0.03	81.1 ± 1.0	88.3 ± 13.3
	Bottom	2.20 ± 0.04	75.6 ± 1.3	125.2 ± 16.7
172	Top	2.41 ± 0.04	82.8 ± 1.3	424.8 ± 24.9
	Middle	2.34 ± 0.04	80.5 ± 1.5	414.9 ± 10.5
	Bottom	2.22 ± 0.04	76.1 ± 1.3	326.7 ± 8.3
173	Top	2.46 ± 0.03	84.6 ± 1.0	100.3 ± 14.2
	Middle	2.35 ± 0.01	80.8 ± 0.3	77.8 ± 8.9
	Bottom	2.11 ± 0.03	72.4 ± 1.0	61.8 ± 7.8
174	Top	2.51 ± 0.03	86.2 ± 0.9	419.3 ± 24.4
	Middle	2.44 ± 0.02	83.8 ± 0.7	380.7 ± 4.2
	Bottom	2.31 ± 0.04	79.2 ± 1.4	369.2 ± 11.6
175	Top	2.40 ± 0.01	82.5 ± 0.5	98.0 ± 7.2
	Middle	2.27 ± 0.06	78.0 ± 2.0	401.2 ± 4.9
	Bottom	2.09 ± 0.05	71.9 ± 1.9	286.2 ± 19.6
176	Top	2.50 ± 0.03	85.9 ± 0.9	91.0 ± 2.8
	Middle	2.48 ± 0.05	85.3 ± 1.7	91.1 ± 5.1
	Bottom	2.35 ± 0.01	80.8 ± 0.5	94.1 ± 4.5
177	Top	2.42 ± 0.03	83.1 ± 1.6	138.8 ± 29.5
	Middle	2.35 ± 0.05	80.9 ± 1.7	104.0 ± 8.2
	Bottom	2.13 ± 0.07	73.3 ± 2.6	99.0 ± 21.0
178	Top	2.47 ± 0.01	84.8 ± 0.3	89.1 ± 9.5
	Middle	2.37 ± 0.03	81.5 ± 1.2	82.0 ± 12.4
	Bottom	2.18 ± 0.03	74.9 ± 1.2	74.7 ± 8.3

3.2 INDENTATION TESTING

Indents at 50- and 100-g loads were placed in longitudinally polished fibers and on fiber ends. These impressions were used to calculate fiber hardness values. The average hardness value for the Nicalon fibers for all samples tested was 22.0 ± 0.7 GPa.

The indented areas of the samples were examined using the Hitachi S-800 scanning electron microscope. It was necessary to sputter carbon onto the polished cross sections before SEM examination because of the charging of epoxy mounting material. The dimensions of the impressions were measured from the SEM photos. SEM photomicrographs of impressions are shown in Fig. 6. Calculated interfacial frictional stresses ranged from <1 MPa to >100 MPa; the average values are given in Table 3.

3.3 FRAGMENTED COATINGS ON INDIVIDUAL FILAMENTS

Initial tests were performed on AVCO SCS-6 filaments with only a silicon carbide coating and with a modifying interlayer of pyrolytic carbon. The critical lengths were measured to be 1.67 ± 0.58 mm and 7.46 ± 0.61 mm, respectively. Using a coating fracture strength of ~200 MPa, extrapolated from matrix fracture results recorded during flexure testing, the interfacial shear strengths were calculated to be 3.98 ± 0.37 MPa and 0.89 ± 0.04 MPa. Figure 7 shows fractures as observed through a stereoscopic microscope at 70X.

Tensile testing of the Nicalon fibers was more complex and tedious. Segmented fracturing was observed on a limited portion of the filaments in each fiber bundle. The lengths of the fragments for uncoated tows were 14 ± 2 μm; the coatings on the carbon-coated bundles flaked off and could not be measured. The interfacial frictional stress for uncoated filaments was calculated to be 39 ± 6 MPa.

RAL-176003

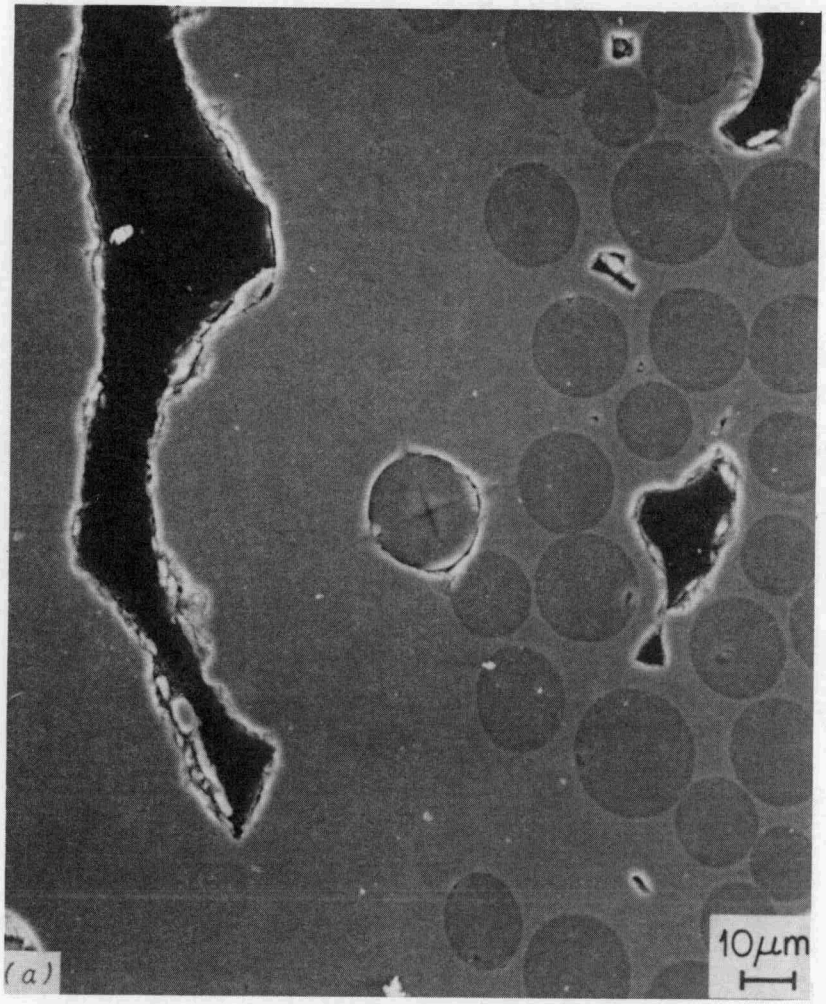

RAL-102743

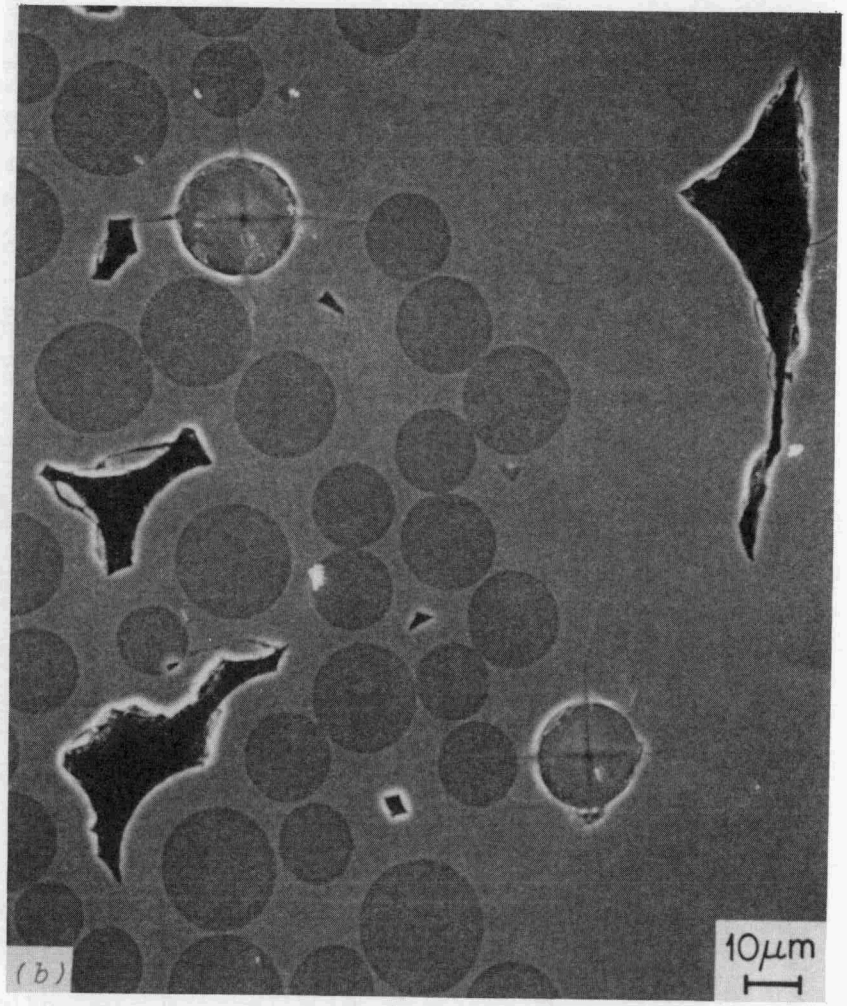

Fig. 6. SEM micrographs showing indented Nicalon fibers. *(a)* CVI-176, Nicalon fibers coated with SiC from methylsilane. *(b)* CVI-178, uncoated Nicalon fibers.

Table 3. Interfacial frictional stress calculated using the indentation method

Sample	Coating	Average fiber diameter (μm)	Frictional stress (MPa)
170	Silicon	16.9 ± 1.2	117.8 ± 60.8
171	Pyrolytic carbon	14.6 ± 2.0	24.7 ± 13.9
172	Boron	16.3 ± 1.3	6.3 ± 1.7
173	Silicon carbide	16.0 ± 1.9	83.9 ± 23.0
174	Pyrolytic carbon	15.4 ± 2.2	0.6 ± 0.4
175	Pyrolytic carbon	13.3 ± 0.7	11.3 ± 4.7
176	Silicon carbide	15.3 ± 0.9	19.9 ± 4.2
177	Boron nitride	15.3 ± 1.9	15.7 ± 5.0
178	Uncoated	16.5 ± 2.4	49.4 ± 14.7

YP-4971

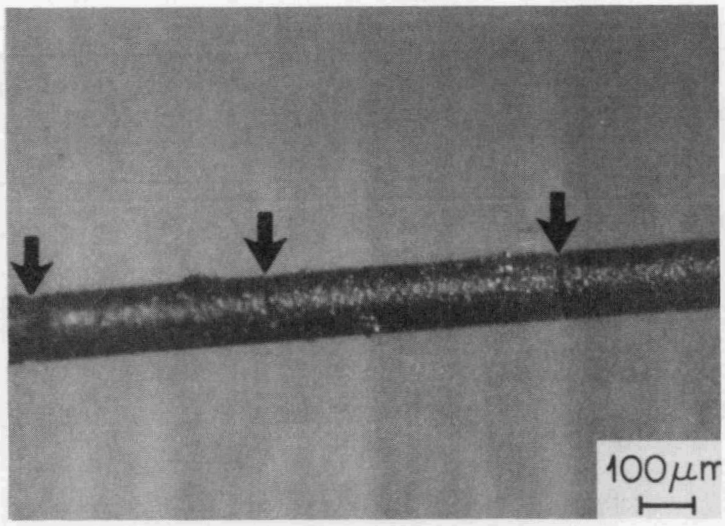

(a)

YP-4970

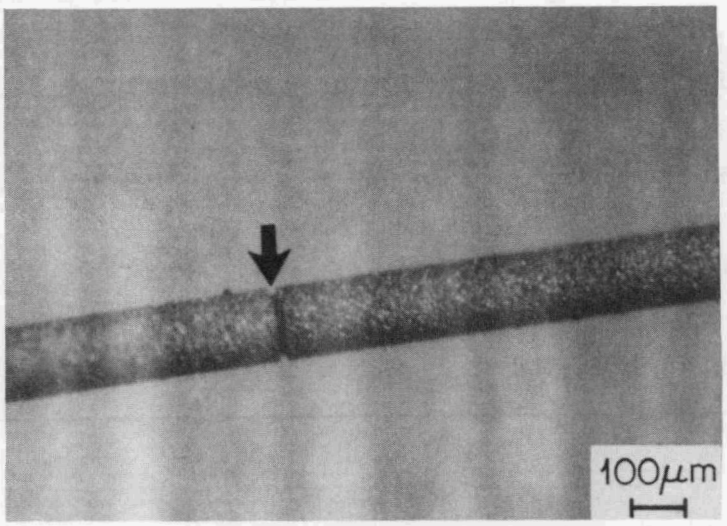

(b)

Fig. 7. Coating fracture observed during testing of AVCO filaments. *(a)* With pyrolytic carbon coating. *(b)* Without interfacial coating.

4. DISCUSSION

4.1 PRECOATING AND FRACTURE BEHAVIOR

In evaluating the mechanical behavior of Nicalon/SiC composites fabricated early in the development of the FCVI process, both brittle and composite fractures were observed in specimens produced under similar conditions. A more thorough analysis employing scanning and transmission electron microscopy revealed the presence of a thin film on the surface of Nicalon fibers in the samples exhibiting fiber pull-out. Initial results and review of other research[6] indicated this layer to possibly be carbonaceous--either a remnant of the sizing or surface enrichment from processing. Auger spectroscopic analysis later showed that the film was composed of silicon and oxygen, possibly as a result of converting the silicon carbide to silicon dioxide during preheating of the fibers prior to infiltration.[28]

The interfacial film could not be detected in the specimens that failed in a brittle manner, suggesting that an intermediate layer may be necessary to obtain fiber pull-out and possibly to protect the fiber from attack during processing. Pyrolytic carbon was chosen to be intentionally applied as an intermediate layer for several reasons. The deposition procedure is chlorine free and requires relatively low temperatures, thus limiting fiber degradation that may be caused by environmental factors. The diffusion rate of carbon into silicon carbide is extremely low, and coating parameters can be adjusted to produce laminar structures in the films that lie parallel to the fibers, enhancing slip.[29,30] The use of a pyrolytic carbon interface coating did result in enhanced mechanical behavior and improved reproducibility.[12]

The influence of the thickness of the pyrocarbon layer on the mechanical behavior of the composite sample was investigated. The concentration of reactant propylene was varied to produce films that ranged in thickness from 0.03 to 0.12 μm. The thickness of the interfacial film had a significant effect on the strength and fracture of the specimens. The interfacial frictional stress was found to be inversely proportional to

the coating thickness. Figure 8 displays the load displacement curves and SEM photographs of fracture surfaces for the carbon-coated composites. The thickest layers produced the most desirable results, a combination of higher strength and large strain to failure.

The usefulness of pyrolytic carbon is limited by its low resistance to oxidation. The carbon layer may also provide excessive slip, thus reducing the usable strength. Other thin films with different bonding and oxidation characteristics were used to modify the fiber-matrix interface and alter the mechanical behavior of the resulting composite body.

Elemental silicon was used as an interface layer because it was thought that diffusing silicon into the fiber would improve the stability of Nicalon. Thermodynamic calculations have been used to show that elemental silicon could react with the excess oxygen and carbon present in the fiber,[31] preventing the formation and subsequent degassing of carbon monoxide upon heating of the fibers. A thin silicon film could also oxidize at high temperatures to form a viscous glass that would heal cracks in the composite structure and prevent further oxygen penetration. However, silicon readily diffuses into silicon carbide and increases the chemical interaction and bonding at the interface.

Another approach was to deposit a silicon carbide film from a chlorine-free precursor to protect the fibers from chemical corrosion by HCl or chlorine during densification. Therefore, a thin protective layer of SiC was deposited on the Nicalon preforms from a mixture of methylsilane and argon.

Both the sample composed of uncoated fibers and the composites prepared from preforms treated with thin films of elemental silicon and SiC exhibited low flexure strength. Load-deflection curves and photomicrographs of the fracture surface of these composites are shown in Fig. 9. The specimens displayed completely brittle failure, with no signs of toughening. The lack of fiber pull-out and the flat smooth fracture of the fibers suggest complete failure of the reinforcement and a high degree of bonding. Indentation measurements confirmed the high interfacial frictional stresses; in some cases, the loads were enough to cause splitting of the fiber and extensive cracking of the surrounding matrix.

ORNL-DWG 87-14915R3

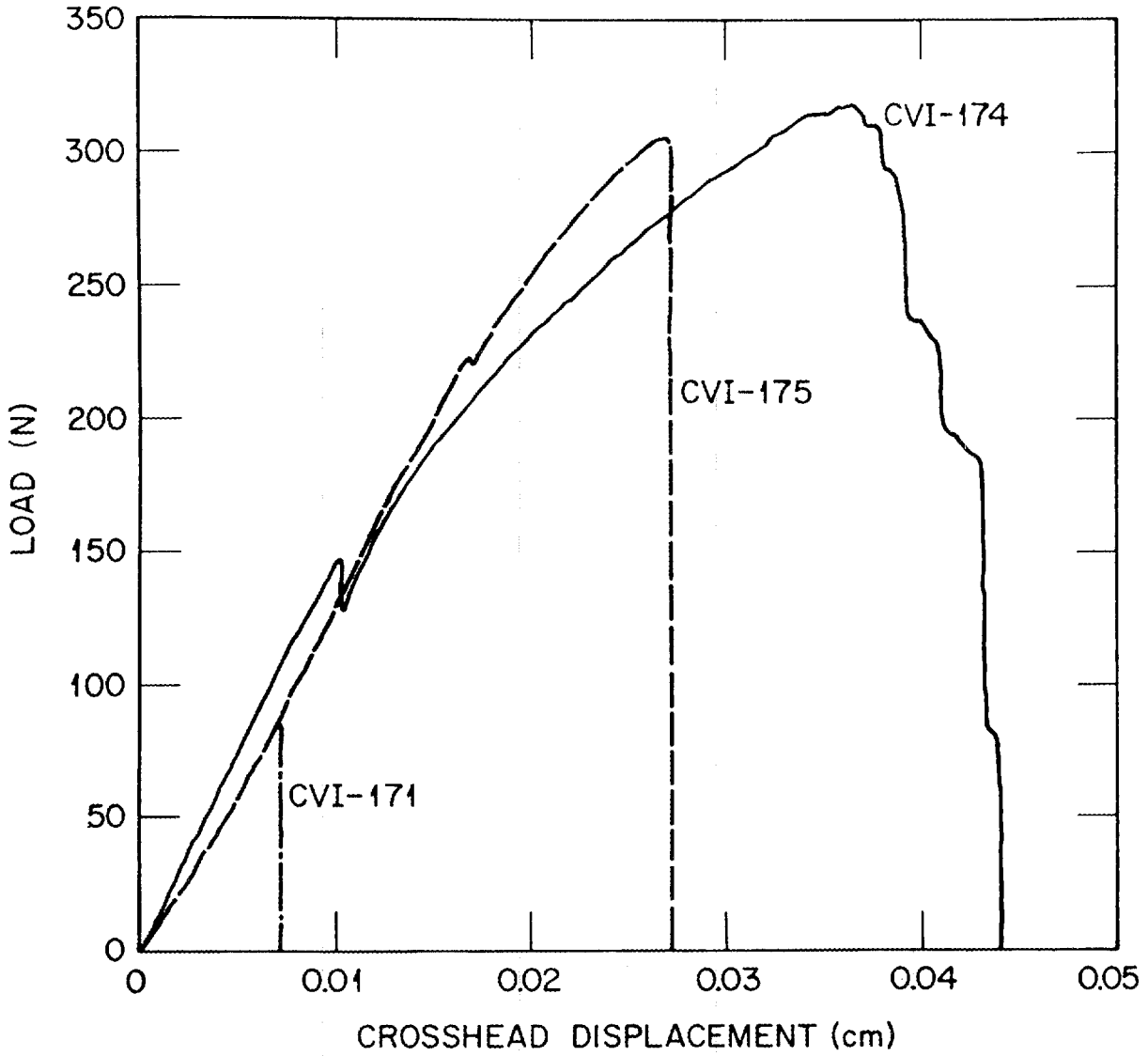

Fig. 8. The effect of varying thickness of pyrocarbon on the fracture of SiC composites. The thicknesses of the pyrolytic carbon coatings on the samples are (*a*) CVI-171 at 0.03 m, (*b*) CVI-175 at 0.07 m, and (*c*) CVI-174 at 0.12 m.

RCM-4337

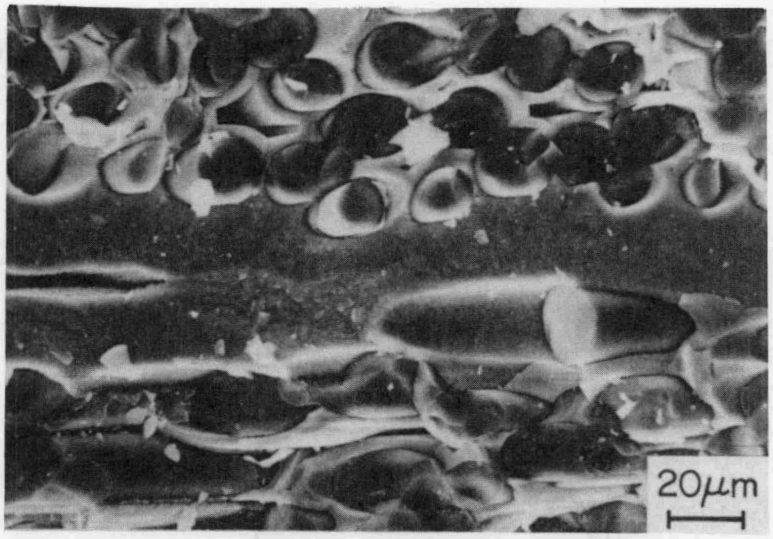

(a)

RAL-175203

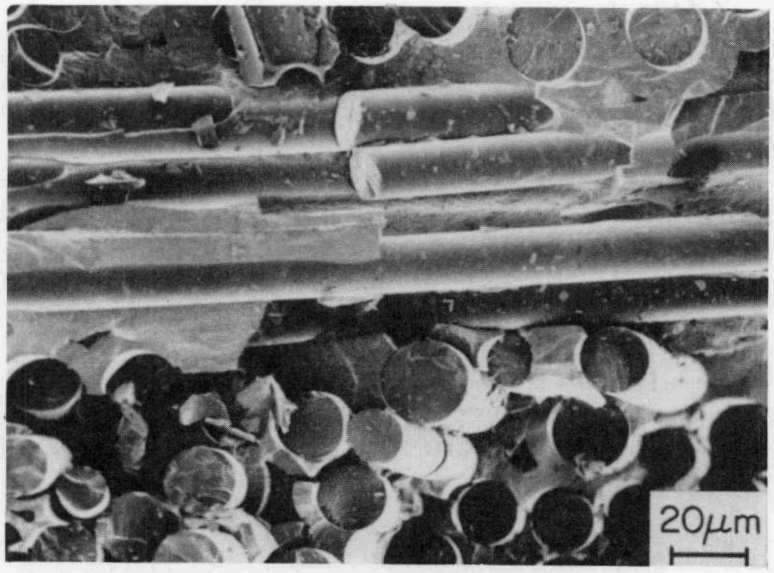

(b)

Fig. 8 (cont.)

RCM-4346

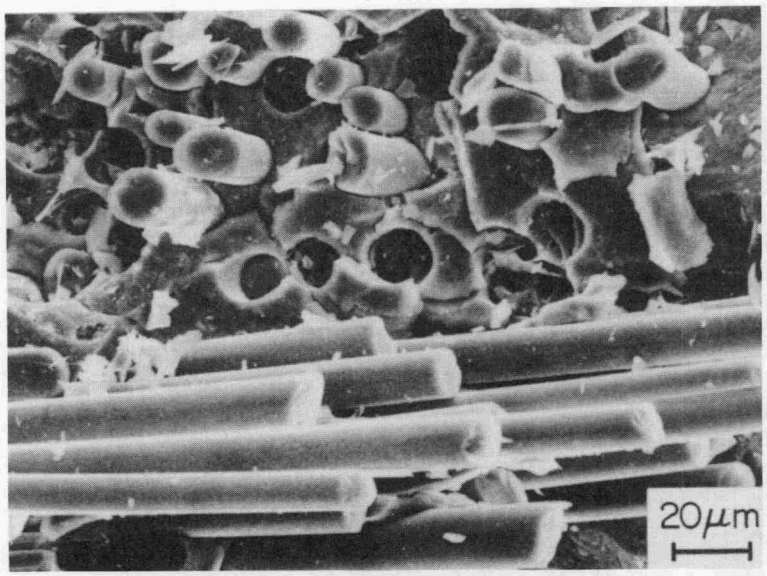

(c)

Fig. 8 (cont.)

ORNL-DWG 87-15949R

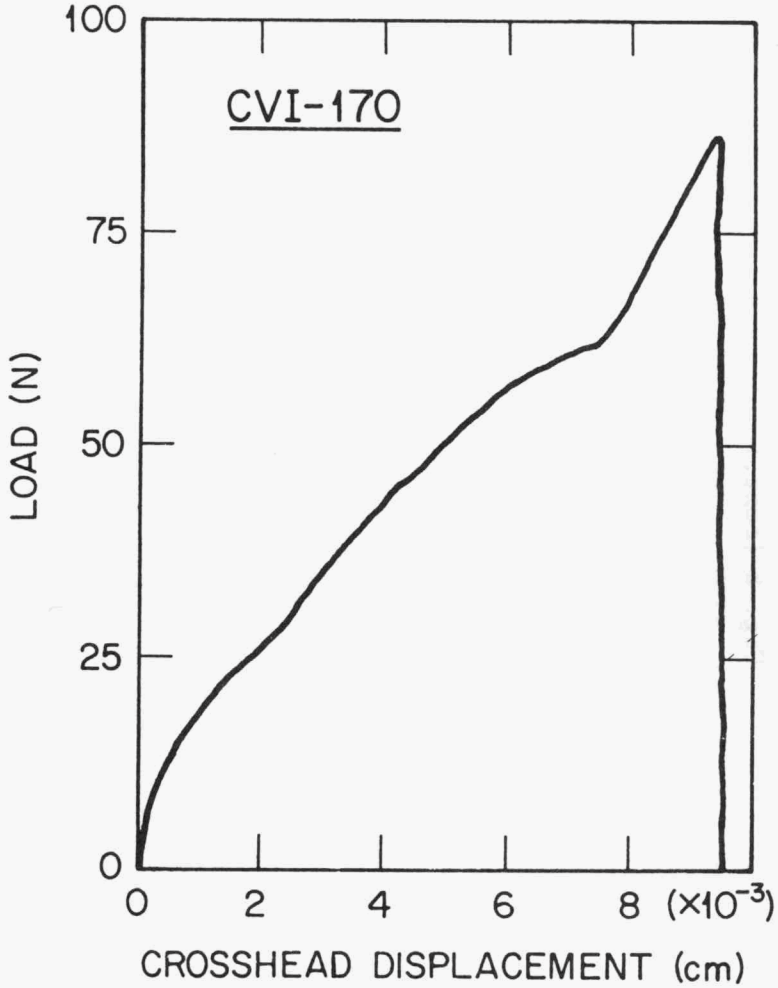

(a)

RCM-4334

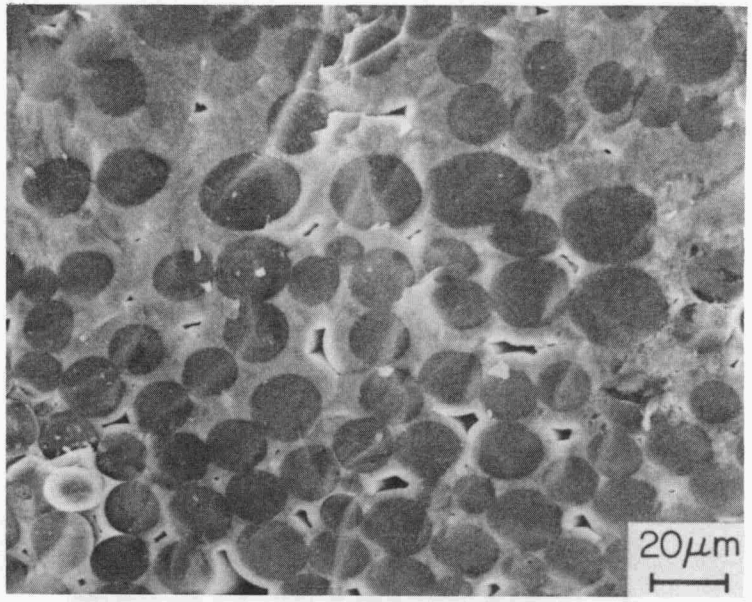

Fig. 9. Load-displacement curves and fracture surfaces of samples containing Nicalon fibers coated with silicon-based compounds. *(a)* CVI-170, silicon coating. *(b)* CVI-173, SiC from methylsilane. *(c)* CVI-176, SiC from methylsilane. *(d)* CVI-178, uncoated fibers.

ORNL-DWG 87-16292R

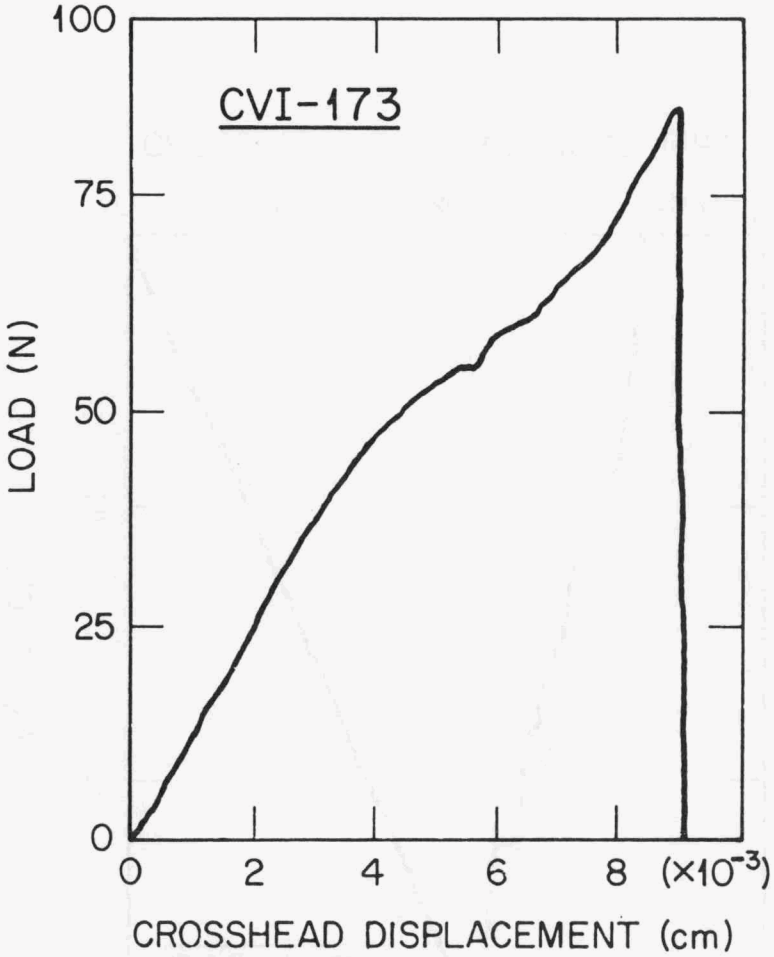

RCM-4343

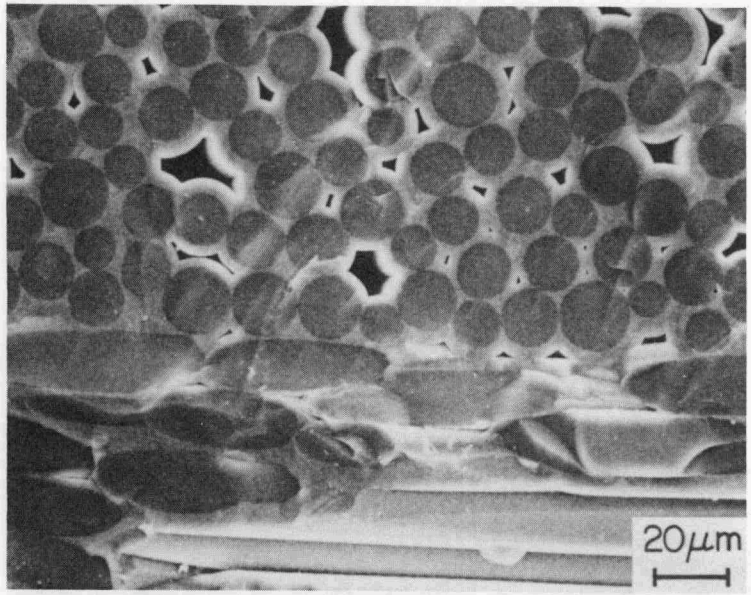

Fig. 9 (Cont.)

(b)

ORNL-DWG 87-18229

RCM-4352

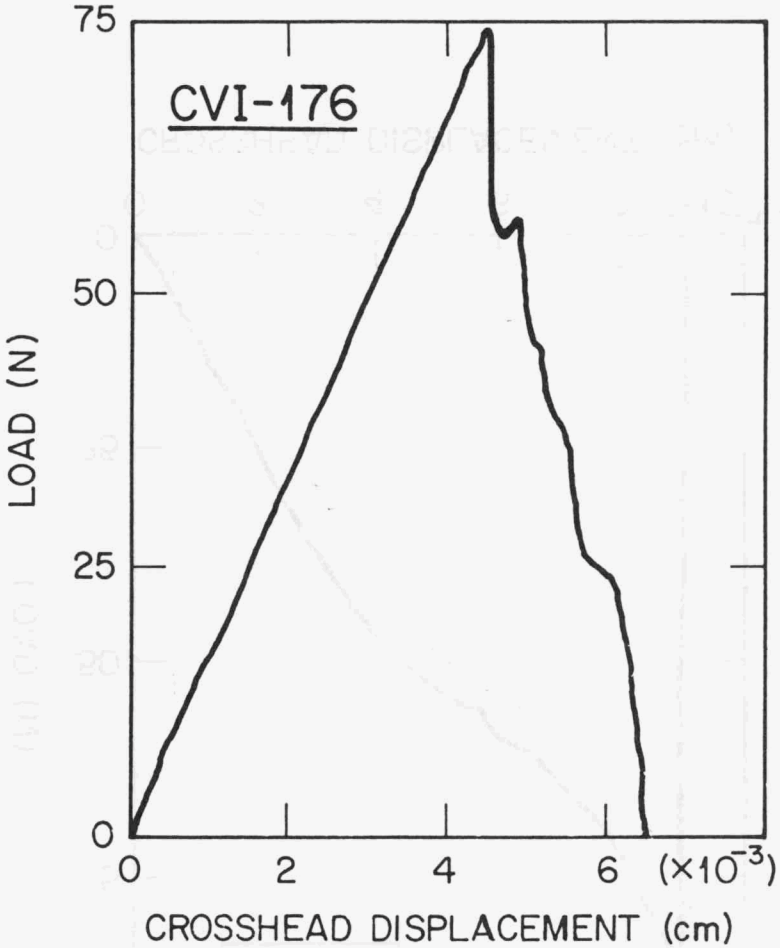

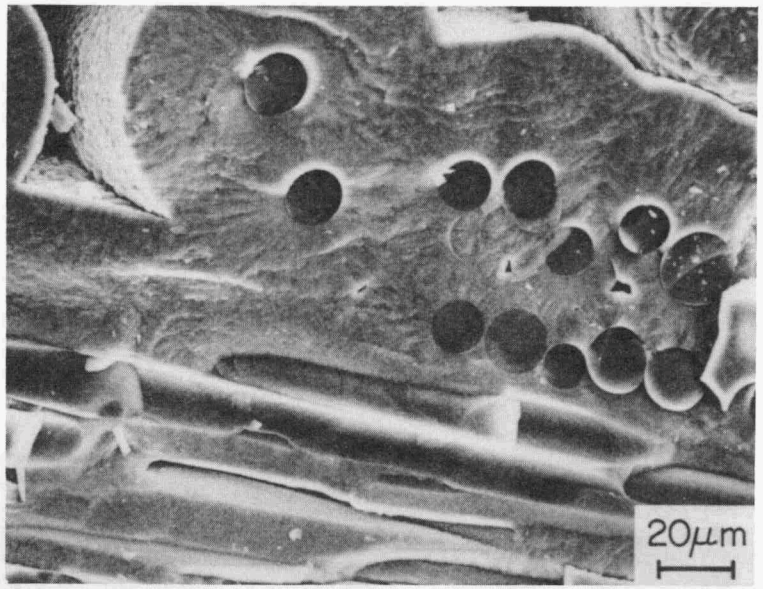

Fig. 9 (Cont.)

(c)

ORNL-DWG 87-15948R

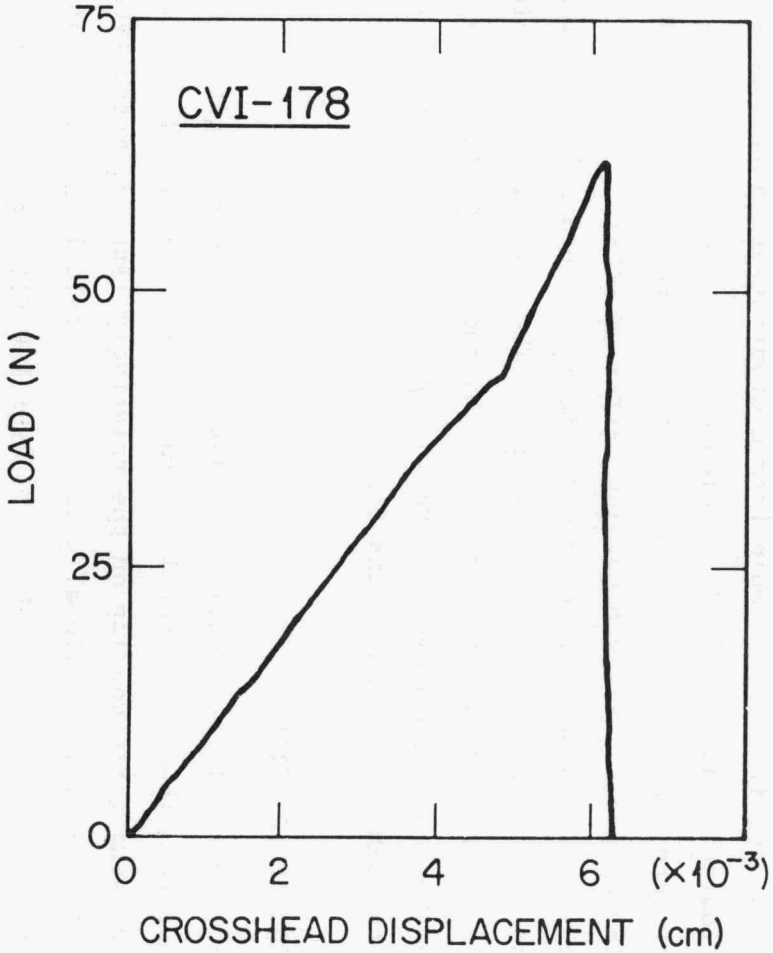

RCM-4358

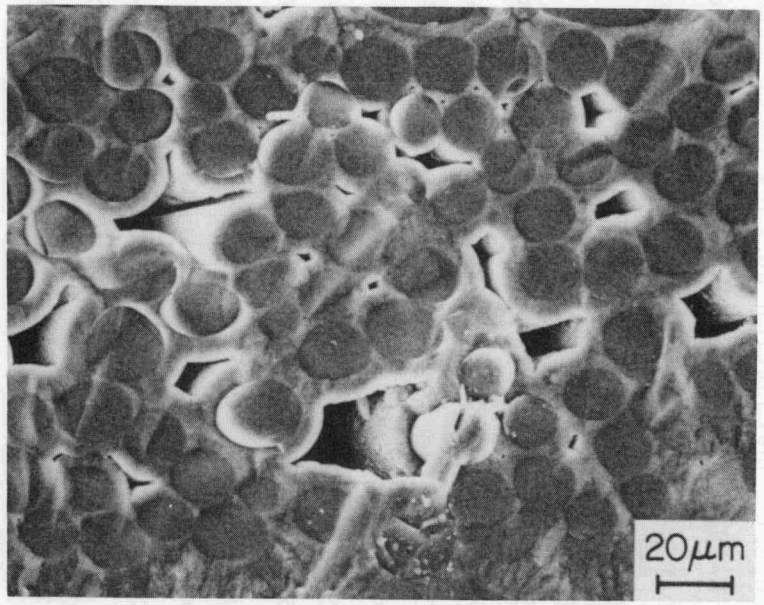

Fig. 9 (Cont.)

(*d*)

The intense bonding and fiber property degradation appears to be a result of silicon diffusion into the fiber from the interface coating or matrix material. It becomes obvious that a chemically inert coating is needed to modify the fiber-matrix bonding and simultaneously protect the fiber reinforcement from processing environments.

Boron nitride has been employed as a modifying interlayer in various composite systems.[10,11] Submicron boron nitride coatings have been proved to be valuable in controlling fiber-matrix bonding and interaction in zircon and zirconium titanate composites, as well as in other glass matrix systems. The graphite-like properties of boron nitride combined with its chemical inertness make it an excellent alternative to carbon for use in oxide-based systems in which carbon would react with oxide fiber or matrix at elevated temperature. Like carbon, boron nitride lacks resistance to oxidation at elevated temperatures. A sample precoated with boron nitride from a diborane/ammonia mixture exhibited low strength and limited fiber pull-out. The calculated frictional stress of 15.7 ± 5.0 MPa is moderate relative to the other composite samples.

Boron was deposited on a sample from a diborane/argon mixture at a relatively low temperature, 775 K. Elemental boron, which closely resembles silicon, has a melting point of 2575 K. Boron, however, does not readily diffuse into the silicon carbide matrix or fibers.[32] At higher temperatures in air, a boron layer would oxidize to form a low melting point glass that would act as a crack sealer. The composite containing the boron-coated fibers had high flexure strengths and reasonable strain, as depicted by the load-displacement curve in Fig. 10. Fiber pull-out is evident in the SEM photograph in the figure.

4.2 INTERFACIAL FRICTION

The usefulness of the tensile test described in this report as a semiquantitative method for determining interfacial frictional stresses was demonstrated using a SiC coating on the relatively large diameter AVCO SiC filaments. Interfacial frictional stresses were calculated from measured critical lengths for systems with and without a modifying interlayer. The low magnitude of the values is supported by the delamination of the

ORNL-DWG 87-14916R2

RCM-4340

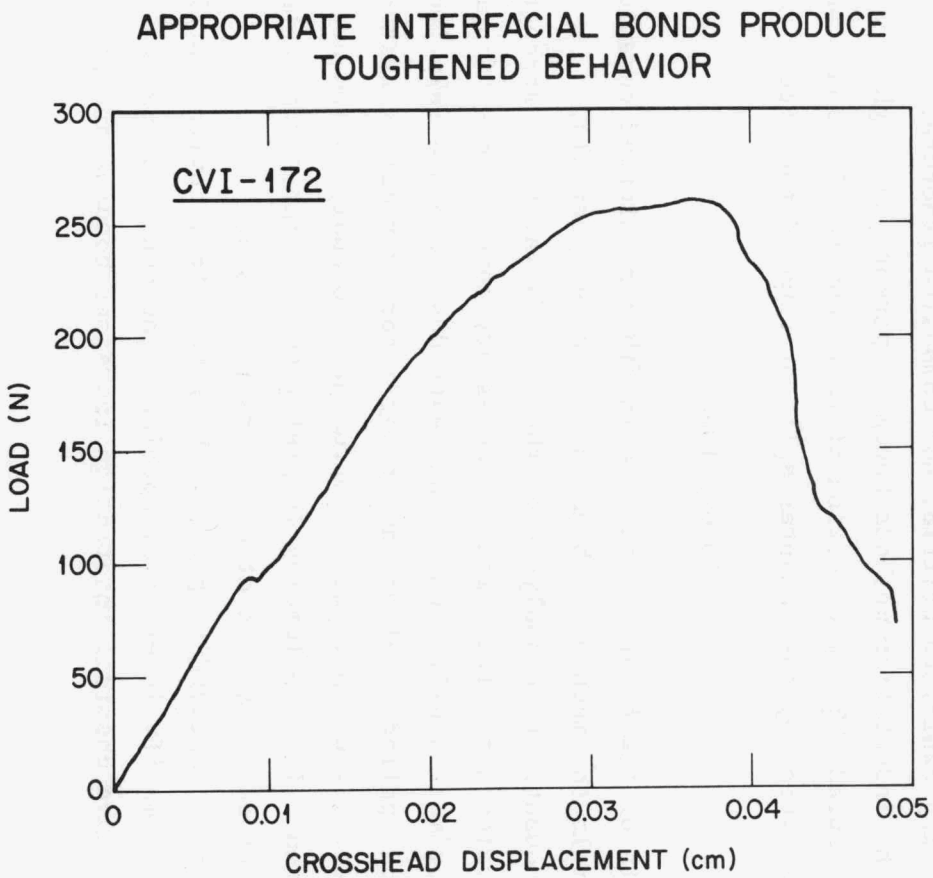

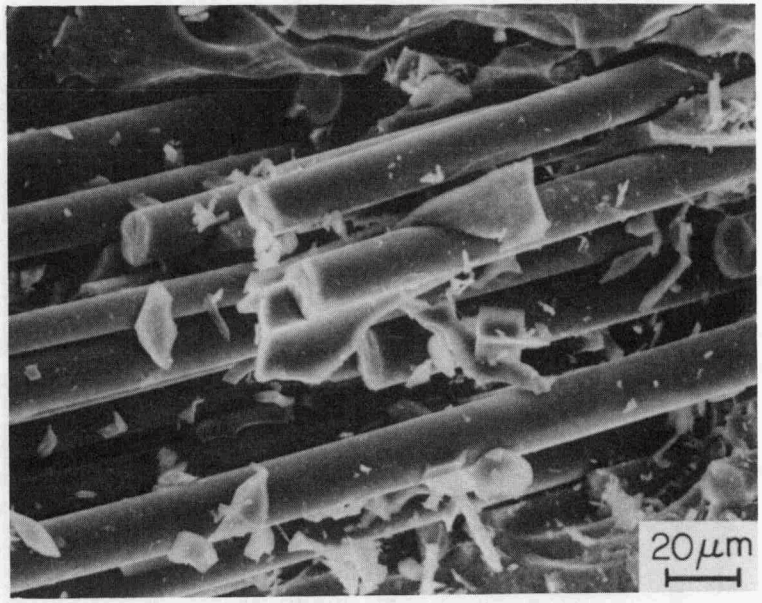

Fig. 10. Boron overcoating provided a favorable combination of strength and pull-out.

composites and debonding of the individual filaments from the matrix observed during four-point flexure testing of composites formed from these fibers.

The tensile test is dependent upon producing a reproducible coating with a known rupture stress. In this analysis, the strength of the coating was extrapolated from mechanical property test results for over 50 CVI SiC/Nicalon composites. A fiber modulus of 180 GPa was obtained from the literature.[33-36] The hardness of 22.0 ± 0.7 GPa, calculated from indent impressions, is high compared with a reported value of 13 GPa.[13] Crystallization of Nicalon, which occurs upon heating above 1475 K, would explain the increase in the hardness value.[33]

The values for interfacial frictional stress were relatively high: 39 MPa, determined from fracture lengths, and 49.4 MPa, calculated from indent measurements, for SiC on uncoated Nicalon. In comparison, reported shear numbers for Nicalon/glass composites are ~2.0 MPa.[13] Reported values are consistent with observed behavior, because Nicalon/SiC composites with no interface coating exhibited brittle, non-composite fracture. The limitations of the indentation methods become apparent when high shear strengths are measured. The application of large compressive loads on the fiber ends as delivered by the indenter split or crushed the fiber.

5. CONCLUSIONS

The strength of the fiber-matrix bond in fiber-reinforced ceramic composites controls the mechanical behavior of these materials. Qualitative and quantitative analyses of the interfacial shear strength is essential to develop composites with the necessary combinations of strength and toughness for most applications. The tests described are relatively simple and can be applied to almost any fiber-interlayer-matrix system. They employ relatively uncomplicated instruments and analyses and are easily implemented. Tensile loading is preferred to compression in testing because failure of ceramics most often occurs in tension.

Coatings can be employed to protect the fibers from environmental degradation and to modify interfacial bonding. The coatings must be inert to the fibers because chemical interaction increases bonding and reduces

fiber strength. The strongest composites with the largest displacement to failure resulted from the thickest precoats. The fibers were well protected from chemical attack, and the materials provided adequate bonding and slip.

Continuing development will be aimed at employing a fixture to observe smaller filaments in an SEM while applying the load. The method is versatile and rather uncomplicated; it can be applied to a large number of fiber-interlayer-matrix systems more easily than other techniques. After quantitative analysis of interfacial frictional strengths is complete, the fiber-matrix bond can be modified to achieve desired combinations of strength and fracture toughness in composite materials.

6. ACKNOWLEDGMENTS

The authors recognize R. C. Melton for some fine electron microscopy and R. D. Cole for assistance in physical property measurements. Appreciation is due L. F. Allard and M. A. Janney for manuscript review, and D. L. Balltrip, D. J. Walmsley, and P. H. Wilson for preparation for publication.

7. REFERENCES

1. P. J. Lamicq et al., "SiC/SiC Composite Ceramics," *Am. Ceram. Soc. Bull.* 65(2), 336-38 (1986).

2. K. M. Prewo and J. J. Brennan, "High-Strength Silicon Carbide Fiber-Reinforced Glass-Matrix," *J. Mater. Sci.* 15, 463-8 (1980).

3. D. P. Stinton, A. J. Caputo and R. A. Lowden, "Synthesis of Fiber-Reinforced SiC Composites by Chemical Vapor Infiltration," *Am. Ceram. Soc. Bull.* 65(2), 347-50 (1986).

4. M. A. Herron and S. H. Risbud, "Characterization of SiC-Fiber-Reinforced Ba-Si-O-N Glass-Ceramic Composites," *Am. Ceram. Soc. Bull.* 65(2), 342-46 (1986).

5. R. W. Rice, "Mechanisms of Toughening in Ceramic Matrix Composites," *Ceram. Eng. Sc. Proc.* 2(7-8), 661-701 (1981).

6. D. B. Marshall and A. G. Evans, "Failure Mechanisms in Ceramic-Fiber/Ceramic-Matrix Composites," *J. Amer. Ceram. Soc.* **68**(5), 225-31 (1985).

7. B. Budiansky, J. W. Hutchinson, and A. G. Evans, "Matrix Fracture in FIber-Reinforced Ceramics," *J. Mech. Phys. Solids* **34**(2), 167-89 (1986).

8. V. R. Riley and J. L. Reddaway, "Tensile Strength and Failure Mechanics of Fiber Composites," *J. Mat. Sci.* **3**, 41-46 (1968).

9. D. C. Phillips, "Interfacial Bonding and the Toughness of Carbon Fibre Reinforced Glass and Glass-Ceramics," *J. Mat. Sci.* **9**, 1847-54 (1974).

10. R. W. Rice et al., "The Effect of Ceramic Fiber Coatings on the Room-Temperature Behavior of Ceramic-Fiber Composites," *Ceram. Eng. Sci. Proc.* 2(7-8), 661-701 (1981).

11. B. Bender et al., "Effect of Fiber Coatings and Composite Processing of Properties of Zirconia-Based Matrix SiC Fiber Composites," *Am. Ceram. Soc. Bull.* **65**(2), 363-9 (1986).

12. A. J. Caputo et al., "Fiber-Reinforced SiC Composites with Improved Mechanical Properties," *Am. Ceram. Soc. Bull.* **66**(2), 268-72 (1987).

13. D. B. Marshall, "An Indentation Method for Measuring Matrix-Fiber Frictional Stresses in Ceramic Components," *Comm. Amer. Ceram. Soc.* C259-60 (December 1984).

14. A. J. Caputo, R. A. Lowden, and D. P. Stinton, *Improvements in the Fabrication of Ceramic-Fiber-Ceramic-Matrix Composites by Chemical Vapor Deposition*, ORNL/TM-9652, June 1985.

15. D. P. Stinton, A. J. Caputo, and R. A. Lowden, "Synthesis of Fiber-Reinforced SiC Composites by Chemical Vapor Infiltration," *Am. Ceram. Soc. Bull.* **65**(2), 347-50 (1986).

16. R. A. Lowden et al., *Effects of Infiltration Conditions on the Properties of SiC/Nicalon Composites*, ORNL/TM-10403, May 1987.

17. A. Takaku and R. C. G. Arridge, "The Effects of Interfacial Radial and Shear Stress on Fiber Pull-Out in Composite Materials," *J. Phys. D: Appl. Phys.* **6**, 2038-47 (1973).

18. C. Atkinson et al., "The Rod Pull-Out Problem, Theory and Experiment," *J. Mech. Phys. Solids* **30**(3), 97-120 (1982).

19. D. B. Marshal and W. C. Oliver, "Measurement of Interfacial Mechanical Properties in Fiber-Reinforced Ceramic Composites," *J. Am. Ceram. Soc.* **70**(8), 542-8 (1987).

20. M. F. Doerner and W. D. Nix, "A Method for Interpreting the Data from Depth Sensing Indentation Instruments," *J. Mater. Res.* **1**(4), 601-9 (July/August 1986).

21. W. C. Oliver, "Progress in the Developments of a Mechanical Properties Microprobe," *MRS Bulletin*, 15-19 (September/October 1986).

22. S. Shojiro and K. Osamura, "Stress Distribution in a Segmented Film on Metal Fiber Under Tensile Loading," *J. Mater. Sci.* **21**, 2744-52 (1986).

23. S. Shojiro and K. Osamura, "A Study of Multiple Fracture Phenomenon of a Coating Film on a Metal Fiber by Means of a Computer Simulation," *J. Mater. Sci.* **21**, 2735-43 (1986).

24. S. Shojiro and K. Osamura, "A Computer Simulation of Strength of Metal Matrix Composites with a Reaction Layer at the Interface," *Met. Trans.* **18A**, 673-79 (April 1987).

25. J. Aveston, G. A. Cooper and A. Kelly, "Single Multiple Fracture: The Properties of Fiber Composites," *National Physics Lab Conference Proceedings* (November 1971).

26. J. Aveston and A. Kelly, "Theory of Multiple Fracture of Fibrous Composites," *J. Mat. Sci.* **8**, 352-62 (1973).

27. L. T. Drzal et al., "Interfacial Shear Strength and Failure Mechanisms in Graphite Fiber Composites," *Proceedings of the 35th Annual Technical Conference*, 1980, Reinforced Plastics/Composites Institute, The Society of the Plastics Industry, Inc.

28. M. H. Rawlins et al., "Interfacial Characterization of Fiber-Reinforced SiC Composites Exhibiting Brittle and Toughened Fracture Behavior," *MRS Symposium Proceedings*, Vol. 78, Advanced Structural Ceramics (November 1986).

29. W. V. Kotlensky, "Deposition of Pyrolytic Carbon in Porous Solids," *Chem. Phys. Carbon* **9**, 173-262 (1973).

30. H. O. Pierson and M. L. Lieberman, "The Chemical Vapor Deposition of Carbon on Carbon Fibers," *Carbon* **13**, 159-66 (1975).

31. K. L. Luthra, "Thermochemical Analysis of the Stability of Continuous 'SiC' Fibers," *J. Am. Ceram. Soc.* **69**(10), C231-3 (1986).

32. Y. A. Vodakov et al., "Diffusion of Boron and Aluminum in n-SiC," *Soviet Physics-Solid State* **8**(4), 1040-1 (1966).

33. G. Simon and A. R. Busnell, "Creep Behavior and Structural Characterization at High Temperatures of Nicalon SiC Fibers," *J. Mater. Sci.* **19**, 3658-70 (1984).

34. G. Simon and A. R. Busnell, "Mechanical and Structural Characterization of the Nicalon Silicon Carbide Fiber," *J. Mater. Sci.* 19, 3649-57 (1984).

35. T. Mah et al., "Thermal Stability of SiC Fibers (Nicalon)," *J. Mater. Sci.* **19**, 1191-201 (1984).

36. C. H. Anderson and R. Warren, "Silicon Carbide Fibers and Their Potential Use In Composite Materials. Part 1," *Composites* **15**(1), 16-24 (1984).

INTERNAL DISTRIBUTION

1-2. Central Research Library
3. Document Reference Section
4-5. Laboratory Records Department
6. Laboratory Records, ORNL RC
7. ORNL Patent Section
8. L. F. Allard
9. P. Angelini
10. R. L. Beatty
11. T. M. Besmann
12. R. A. Bradley
13. A. J. Caputo
14. R. H. Cooper
15. D. R. Johnson
16. R. R. Judkins
17. E. L. Long, Jr.
18-22. R. A. Lowden
23. T. A. Nolan
24. W. C. Oliver
25. R. E. Pawel
26. A. C. Schaffhauser
27. M. A. Schmidt
28-32. D. P. Stinton
33-35. P. T. Thornton
36. J. R. Weir
37. H. D. Brody (Consultant)
38. G. Y. Chin (Consultant)
39. F. F. Lange (Consultant)
40. W. D. Nix (Consultant)
41. D. P. Pope (Consultant)
42. E. R. Thompson (Consultant)

EXTERNAL DISTRIBUTION

43. ACUREX CORPORATION, 555 Clyde Avenue, P.O. Box 7555, Mountain View, CA 94039

J. Sawyer

44. ADIABATICS, INCORPORATED, 630 S. Mapleton, Columbus, IN 47201

Roy Kamo, President

45-46. AFWAL/MLLM, Wright-Patterson AFB, OH 45433

Alan Katz
S. Szaruga

47-50. AIR PRODUCTS AND CHEMICALS, INC., P.O. Box 538T, Allentown, PA 18105

P. N. Dyer
V. L. Magnotta
R. K. Malhotra
S. V. Raman

51. AIRCO TEMESCAL, 2850 Seventh Street at Heinz, Berkeley, CA 94710

Ernest Demiray

52. AIRESEARCH MANUFACTURING COMPANY, 2525-T West 190th Street, Torrance, CA 90509

D. M. Kotchick

53. AMERCOM, INC., 8928 Fullbright Avenue, Chatsworth, CA 91311

W. E. Bustamante

54. ARCO CHEMICALS COMPANY, Silag Operation, Route 6, Box A, Greer, SC 29651

J. F. Rhodes

55. ARGONNE NATIONAL LABORATORY, 9700 South Cass Avenue, Argonne, IL 60439

W. A. Ellingson

56-57. ARMY MATERIALS AND MECHANICS RESEARCH CENTER, Arsenal Street, Watertown, MA 02172

R. N. Katz
J. W. McCauley

58. AVCO, 201 Lowell Street, Wilmington, MA 01887

Tom Vasilos

59-62. AVCO SPECIALTY MATERIALS, 2 Industrial Avenue, Lowell, MA 01851

B. Belason
T. F. Foltz
W. Foulds
J. F. Lacouste

63-66. BABCOCK & WILCOX COMPANY, Lynchburg Research Center, P.O. Box 239, Lynchburg, VA 24505

L. J. Ferrell
W. G. Long
H. H. Moeller
D. R. Petrak

67-68. BATTELLE COLUMBUS LABORATORIES, 505 King Avenue, Columbus, OH 43201

S. P. Mukherjee
I. G. Wright

69-72. BATTELLE PACIFIC NORTHWEST LABORATORIES, P.O. Box 999, Battelle Boulevard, Richland, WA 99352

Ed Cartwright
T. D. Chikalla
S. D. Dahlgren
Ed McClanahan

73. CABOT CORPORATION, 125 High Street, Boston, MA 02110

Nicholas Fiore

74-76. CATERPILLAR TRACTOR COMPANY, Peoria, IL 61629

M. B. Beardsky
M. Haselkorn
G. G. Volbert

77-78. CERAMATEC, INC., 163 West 1700 Street, Salt Lake City, UT 84115

C. W. Griffin
D. W. Richerson

79-82. CORNING GLASS WORKS, Corning, NY 14831

K. Chyung
R. C. Doman
D. C. Larson
P. Papa

83-85. CUMMINS ENGINE COMPANY, INC., 1000 5th St., Columbus, IN 47201

J. W. Patten
G. L. Starr
T. M. Yonushonis

86. DOW CORNING CORPORATION, 3901 South Saginaw Road, Midland, MI 48640

H. W. Foglesong

87-88. E. I. DUPONT DE NEMOURS & COMPANY, INC., Experimental Station 302/22, Wilmington, DE 19898

P. Geoghegan
J. C. Romine

89-90. FORD MOTOR COMPANY, Engineering and Research, P.O. Box 2053, Dearborn, MI 48121

D. L. Hartsock
A. F. McLean

91-92. GA TECHNOLOGIES, INC, P.O. Box 81608, San Diego, CA 92138

T. D. Gulden
K. S. Mazdiyasni

93. GENERAL MOTORS CORPORATION, Allison Gas Turbine Operations, Low Heat Rejection Diesel Technology, P.O. Box 420, Indianapolis, IN 46206

H. E. Helms

94-95. GEORGIA INSTITUTE OF TECHNOLOGY, 225 North Avenue, Atlanta, GA 30332

W. J. Lackey
T. L. Starr

96-98. GTE LABORATORIES, INC., 40 Sylvan Road, Waltham, MA 02254

M. L. Huckabee
A. E. Pasto
V. Sarin

99. HUGHES AIRCRAFT COMPANY, P.O. Box 902, 2000 East El Segundo Boulevard, El Segundo, CA 90245

Mike Gardos

100. KAMAN SCIENCES CORPORATION, 1500 Garden of the Gods Road, P.O. Box 7463, Colorado Springs, CO 80933

J. L. Carr

101-102. KENNAMETAL, INC., P.O. Box 231, Latrobe, PA 15650

D. Kropful
E. J. Oles

103. KRW ENERGY SYSTEMS, P.O. Box 158, Madison, PA 15663

C. A. Andersson, Jr.

104-106. LANXIDE CORPORATION, Tralee Industrial Park, Newark, DE 19711

V. Irick, Jr.
M. Newkirk
A. W. Urquhart

107-109. LAWRENCE BERKELEY LABORATORY, University of California, P.O. Box 808, 1 Cyclotron Road, Berkeley, CA 94720

D. H. Boone
A. G. Evans
A. V. Levy

110-112. LOS ALAMOS NATIONAL LABORATORY, P.O. Box 1663, Los Alamos, NM 87545

F. D. Gac
G. F. Hurley
J. J. Petrovic

113-114. MARTIN MARIETTA LABORATORIES, 1450 South Rolling Road, Baltimore, MD 21227

D. C. Nagle
A. R. C. Westwood

115-116. MASSACHUSETTS INSTITUTE OF TECHNOLOGY, Cambridge, MA 02139

H. K. Bowen
J. S. Haggerty

117-118. MECHANICAL TECHNOLOGY, INC., 968 Albany-Shaker Road, Latham, NY 12110

W. F. Bessler
M. Schreiner

119. NASA-LANGLEY RESEARCH CENTER, MS 188-B, Hampton, VA 23665

D. R. Tenney

120-125. NASA-LEWIS RESEARCH CENTER, 21000 Brookpark Road, Cleveland, OH 44135

C. C. Berndt
D. H. Buckley
S. R. Levine
T. J. Miller
H. B. Probst
Harold Sliney

126. NATIONAL ACADEMY OF SCIENCES, National Materials Advisory Board, Washington, DC 20418

R. M. Spriggs

127-128. NATIONAL BUREAU OF STANDARDS, 562 Fracture and Deformation, Gaithersburg, MD 20899

E. R. Fuller
S. M. Wiederhorn

129. NATIONAL RESEARCH COUNCIL OF CANADA, 1411 Oxford Street, Halifax, N.S., Canada B3H3Z1

K. J. Konsztowicz

130-131. NORTH CAROLINA STATE UNIVERSITY, Department of Materials Engineering, P.O. Box 5427, 232 Riddick Laboratory, Raleigh, NC 27607

Hans Conrad
R. F. Davis

132. NORTH CAROLINA STATE UNIVERSITY, P.O. Box 5995, Raleigh, NC 27607

H. Palmour III

133. OAK RIDGE ASSOCIATED UNIVERSITIES LIBRARY, Oak Ridge, TN 37831

MERT Division

134. OHIO STATE UNIVERSITY, 2041 College Road, Columbus, OH 43210

Dennis Readey

135-136. PENNSYLVANIA STATE UNIVERSITY, Materials Engineering Research Laboratory, 201 Steidle Building, University Park, PA 16802

Karl Spear
R. E. Tressler

137-139. PRATT & WHITNEY AIRCRAFT, 400 Main St., East Hartford, CT 06108

O. Chen
C. S. Giggins
D. L. Ruckle

140. REFRACTORY COMPOSITES, INC., 12220-A Rivera Road, Whittier, CA 90606

E. Paquette

141. ROCKWELL INTERNATIONAL, 1049 Camino Dos Rios, P.O. Box 1085, Thousand Oaks, CA 91360

P. E. D. Morgan

142. RUTGERS UNIVERSITY, P.O. Box 909, Bowser Road, Piscataway, NJ 08854

J. B. Wachtman, Jr.

143. SAN FERNANDO LABORATORIES, 10258 Norris Avenue, Pacoima, CA 91331

R. A. Holzl

144. SANDIA NATIONAL LABORATORIES, P.O. Box 5800, Albuquerque, NM 87115

Donald Maddox

145. R. L. Smith, P.O. Box 98, Chassel, MI 49916

146. TECHNOLOGY ASSESSMENT AND TRANSFER COMPANY, 9607 Muirfield Drive, Upper Marlboro, MD 20772

L. L. Fehrenbacher

147. 3M COMPANY, 3M Center, 218-35-04, St. Paul, MN 55144

R. E. Richards

148. UNION CARBIDE CORPORATION, Market Development, Carbon Products Division, P.O. Box 6087, Cleveland, OH 44101

M. B. Dowell

149. U.S. ARMY TANK-AUTOMOTIVE COMMAND (TACOM), R&D Center, Warren, MI 48090

P. C. Glance

150. U.S. DEPARTMENT OF DEFENSE, Advanced Research Projects Agency, 1400 Wilson Boulevard, Arlington, VA 22209

B. F. Wilcox

151-152. UNITED TECHNOLOGIES RESEARCH CENTER, Silver Lane, MS 24, East Hartford, CT 06108

J. J. Brennan
Karl Prewo

153. UNIVERSITY OF TENNESSEE, Department of Materials Science, Knoxville, TN 37996

J. E. Spruill

154. UNIVERSITY OF WASHINGTON, Seattle, WA 98195

R. C. Bradt

155. VIRGINIA POLYTECHNIC INSTITUTE AND STATE UNIVERSITY, Blacksburg, VA 24061

D. P. H. Hasselman

156. VOUGHT CORPORATION, MSTH 83, P.O. Box 225907, Dallas, TX 75265

H. F. Volk

157-158. W. R. GRACE & COMPANY, 7379 Route 32, Columbia, MD 21044

R. W. Rice
J. P. Skalny

159. WESTINGHOUSE ELECTRIC CORPORATION, Research and Development Center, 1310 Beulah Road, Pittsburgh, PA 15235

R. J. Bratton

160-161. WILLIAMS INTERNATIONAL CORPORATION, 2280 West Maple Road, Walled Lake, MI 48088

William Chapman
Peter Nagy

162. DOE, ENERGY CONVERSION & UTILIZATION TECHNOLOGIES DIVISION, Route Symbol CE-142, Forrestal Building, Washington, DC 20545

J. J. Eberhardt

163-164. DOE, MORGANTOWN ENERGY TECHNOLOGY CENTER, P.O. Box 880, Morgantown, WV 26505

D. Dubis
J. S. Wilson

165. DOE, OAK RIDGE OPERATIONS OFFICE, P.O. Box E, Oak Ridge, TN 37831

Office of Assistant Manager for Energy Research and Development

166. DOE, OFFICE OF BASIC ENERGY SCIENCES, Division of Materials Sciences, ER-131, GTN, Washington, DC 20545

F. V. Nolfi

167. DOE, OFFICE OF FOSSIL ENERGY, FE-14, Mail Stop B127, GTN, Washington, DC 20545

F. M. Glaser

168-169. DOE, OFFICE OF VEHICLE AND ENGINE RESEARCH AND DEVELOPMENT, Forrestal Building, 1000 Independence Avenue, Washington, DC 20585

A. A. Chesnes
R. B. Schulz

170. DOE, PITTSBURGH ENERGY TECHNOLOGY CENTER, P.O. Box 10940, Pittsburgh, PA 15236

S. W. Chun

171-200. DOE, TECHNICAL INFORMATION CENTER, Office of Information Services, P.O. Box 62, Oak Ridge, TN 37831

For distribution by microfiche as shown in DOE/TIC-4500, Distribution Categories UC-103 (Fluidized Bed Combustion), UC-105 (Flue Gas Cleanup), UC-106 (Gas Stream Cleanup), UC-108 (Coal Liquefaction), UC-109 [Coal Gasification (Surface and Underground)], UC-110 (Fuel Cells), UC-111 (Heat Engines), and UC-114 (Coal Based Materials and Components).